Optical Modes in a Step-Index Cylindrical Fibre

Team 3: 01849865, 01878398, 02150264

Abstract

The mapping of the supported modes of a **1250 nm signal** (far infrared) in a cylindrical waveguide of **core radius 4.5 microns** with **core refractive index 1.52** and **cladding refractive index of 1.495** is shown. The V-parameter was calculated to be 6.21.

We decided to focus on the **HE_{22} transmission mode**. The field distribution is seen to be shaped like a four-leaf-clover in the core with four lower amplitude antinodes on the cladding-core boundary. The amplitude of the field along the axis of the waveguide (E_z) is an order of magnitude weaker than that of the fields perpendicular to the waveguide axis (E_ϕ and E_r). The effective index is 1.513, propagation constant is 7.53×10^6 m^{-1}, and the proportion of energy transmitted in the core is 88.5%. This means that the signal would face some attenuation and other modes could be more suitable for signal transmission.

A key assumption throughout is that $n_2 \approx n_1$ which allows for simplified electric field equations.

Background

Optical fibres have many applications: [1]

- Telecommunications
- Medical imaging
- Lasers

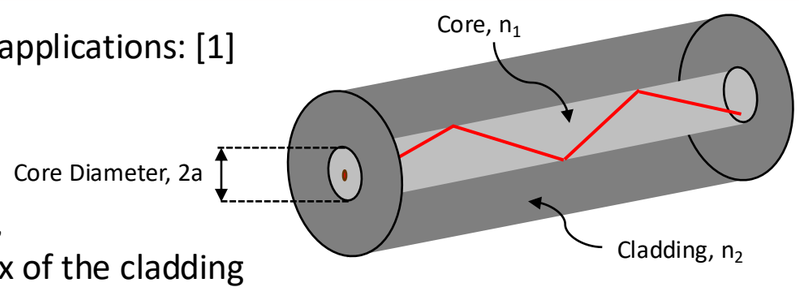

Right is a step index fibre, where the refractive index of the cladding is lower than the core such that total internal reflection occurs and light is guided down the fibre. The modes that are supported depends on:

- core radius, a
- the refractive index of the cladding and core
- the light's wavelength

This work uses numerical methods to explore supported modes' effective indices, propagation constants, fraction of power in the core and waveguide dispersion.

Methods

Finding Supported Modes:

- Find the roots of the equation below using scipy.optimize.fsolve, which finds the roots via a hybrid Powell method [2]

$$J_{m\pm1}(pa) \times qaK_m(qa) \pm K_{m\pm1}(qa) \times paJ_m(pa) = 0$$

- The roots for different values of m can then be used to calculate the effective index and propagation constants of each mode, where the positive version of this equation corresponds to EH modes and the negative version to HE modes.

Plotting E-Fields:

- General method created to input parameters and returns vectors.
- This method was run at discrete interval throughout the waveguide set by fixing the 'density' of the plot.
- The various plots are made by choosing which vectors or combinations to use.

Fraction of power in the core:

- This was calculated by summing the values of intensity in the core regions and dividing by the sum of all intensity values
- The more formal method integrates intensity with respect to area, but this method is similar in concept to approximating an integral as the sum of small rectangle areas.

Waveguide Dispersion:

- $D_W = -\frac{\lambda}{c}\left[\frac{\partial^2 n_{eff}}{\partial \lambda^2}\right]_W = -\frac{\lambda}{c}\left[\frac{\partial^2 n_m}{\partial \lambda^2}\right]_W$
- The second derivative was found by taking the mean of the central difference method for wavelengths at different step sizes around the transmitted wavelength.

Results

Mode	n_{eff}	ß (10^6 m^{-1})	D_w (ps km^{-1} nm^{-1})
HE_{11}	1.517	7.627	6.86 ± 0.01
TE_{01}, TM_{01}, HE_{21}	1.513	7.606	15.12 ± 0.01
EH_{11}, HE_{31}	1.508	7.578	20.60 ± 0.01
HE_{12}	1.506	7.570	13.00 ± 0.01
HE_{41}, EH_{21}	1.501	7.546	11.73 ± 0.03
TE_{02}, TM_{02} ,HE_{22}	1.498	7.530	-106.51 ± 0.80

Table 1: All the modes supported by the fibre, their propagation constant (ß), effective index (n_{eff}) and the waveguide dispersion (D_w). Degenerate modes under $n_2 \approx n_1$ assumption have been grouped together.

Table 1 summarises the supported modes and associated effective index and propagation constant. This fibre supports multiple modes despite a small core radius due to a relatively high V-parameter. The assumption that $n_2 \approx n_1$ has led to degenerate modes that have the same values of n_{eff}, ß and D_w. Waveguide dispersion is caused by variation of ß with λ. Additionally, different modes have different amounts of electric field in the lower refractive index of the cladding, hence differing dispersion values [3]. The TE_{02}, TM_{02}, HE_{22} modes exhibit normal waveguide dispersion, indicated by the negative value, whilst the other modes exhibit anomalous waveguide dispersion.

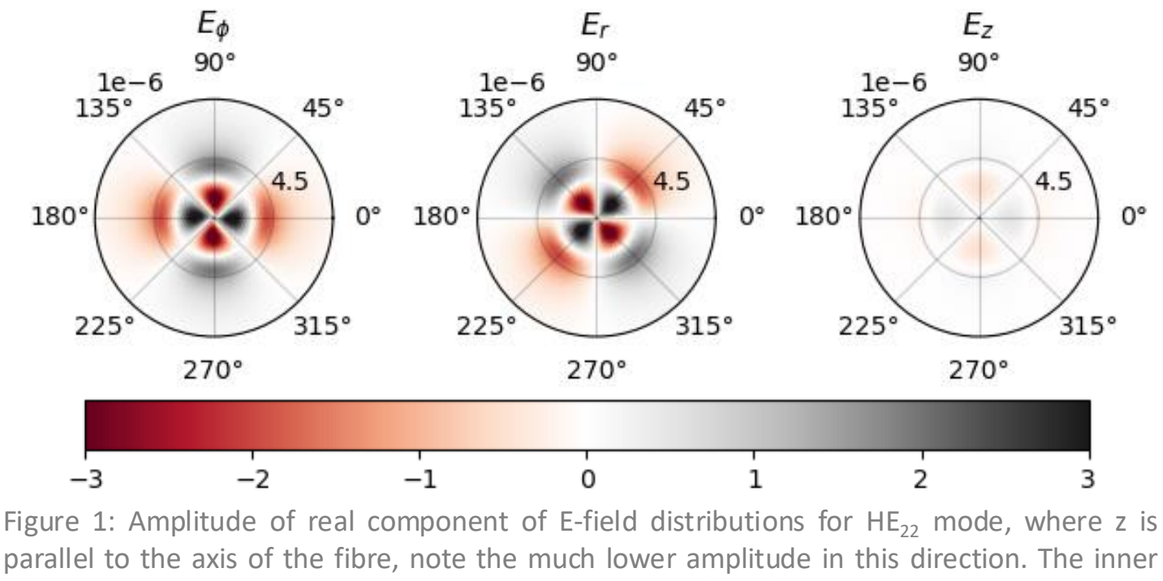

Figure 1: Amplitude of real component of E-field distributions for HE_{22} mode, where z is parallel to the axis of the fibre, note the much lower amplitude in this direction. The inner circle labelled 4.5 of each subplot, represents the edge of the fibre's core.

Above are the different components of electric field for the HE_{22} mode – the amplitude of E_z is much lower as this is not a transverse mode. E_ϕ and E_r are always 45 degrees out of phase. Beyond the pattern that this mode produces, we note that the electric field extends into the cladding of the fibre. This can be seen both in the spatial intensity distribution below, in which there is a slight halo surrounding the core radius, and in HE_{22} having a lower fraction of power in the core (Γ=0.885). Whilst this is a high fraction of power in the core – HE_{11} has Γ=0.995 indicating that this mode is more effectively guided and would experience less losses. [4]

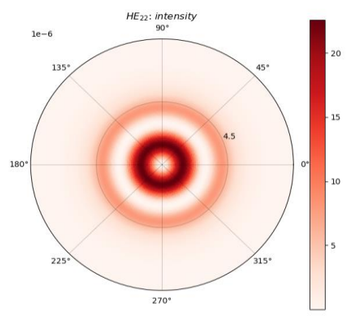

Figure 2: Spatial intensity for HE_{22} mode. The circular grig line labelled 4.5 is at the radius of the core

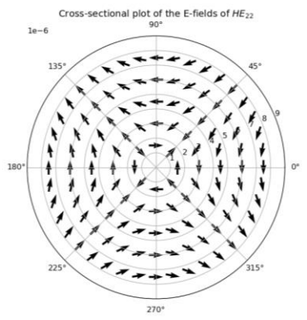

Figure 3: Electric field lines of HE_{22} for fibre cross-section at z = 0.

In Fig. 3, we can see the electric field lines of the HE_{22} mode - note that we see the same lobes present in the amplitude plots. These types of diagram could also be used to interpret polarization, by considering the direction of field lines, though this is easier in the lower order modes.

[1] S. Addanki, I. S. Amiri, and P. Yupapin, "Review of optical fibers-introduction and applications in fiber lasers," vol. 10, pp. 743–750, 2018, doi: 10.1016/j.rinp.2018.07.028.
[2] M. POWELL, "A hybrid method for nonlinear equations," 1970.
[3]D. Large and J. Farmer, *Chapter 4 - Linear Fiber-Optic Signal Transportation*. Boston: Morgan Kaufmann, 2009, pp. 81–126.
[4] D. Tosi, M. Sypabekova, A. Bekmurzayeva, C. Molardi, and K. Dukenbayev, 2 Principles of fibre optic sensors, Academic Press, 2022, pp. 19–78.

Plots of all supported modes